

# Strange particle production in relativistic nucleus-nucleus collisions at RHIC and LHC energy regions<sup>\*</sup>

REN Xiao-Wen(任小文)<sup>1</sup> FENG Sheng-Qin(冯笙琴)<sup>1,2,3;1)</sup> YUAN Xian-Bao(袁显宝)<sup>1</sup>

<sup>1</sup> College of Science, China Three Gorges University, Yichang 443002, China

<sup>2</sup> Key Laboratory of Quark and Lepton Physics (Huazhong Normal University),  
Ministry of Education, Wuhan 430079, China

<sup>3</sup> School of Physics and Technology, Wuhan University, Wuhan 430072, China

**Abstract:** PACIAE, a parton and hadron cascade model, is utilized to systematically investigate strange particle production and strangeness enhancement in Au+Au collisions and in Pb+Pb collisions with the  $\sqrt{s_{NN}}=200$  GeV at the RHIC and 2.76 TeV at the LHC, respectively. The experimental results at different centralities, using data from the STAR collaboration and the ALICE collaboration, are well described by the PACIAE model. This may represent the importance of the parton and hadron rescatterings, as well as the reduction mechanism for strange quark suppression, that are implemented in the PACIAE model.

**Key words:** strange particle, rapidity densities at midrapidity, transverse momentum distribution, PACIAE model

**PACS:** 25.75.Dw, 24.10.Lx **DOI:** 10.1088/1674-1137/38/5/054102

## 1 Introduction

Relativistic heavy ion collisions aim to create a Quark Gluon Plasma (QGP), which is a unique state of matter where quarks and gluons can move freely over volumes that are large in comparison to the typical size of a hadron. Strange particle production and strangeness enhancement in relativistic nucleus-nucleus collisions relative to pp collisions at the same energy have been proposed as a signature of the QGP formation in relativistic heavy ion collisions [1]. This is based on the principle that the threshold energy of strange particle production in QGP is higher than that in hadronic matter. Therefore, the yield of strangeness is a good probe of QGP.

Recently, the ALICE collaboration working at the Large Hadron Collider (LHC) has reported new data for strange particle production in Pb+Pb collisions at  $\sqrt{s_{NN}}=2.76$  TeV [2]. This is a new energy regime for relativistic nucleus-nucleus collisions. Similarly, the STAR collaboration [3] working at the Relativistic Heavy Ion Collider (RHIC) have published results for strange particle production in Au+Au at  $\sqrt{s_{NN}}=200$  GeV. Based on PYTHIA, the PACIAE [4, 5] model is used to analyze strange particle production in relativistic nuclear-nuclear collisions.

In the LUND string fragmentation scheme [6], the

suppression of the s quark pair production compared with u(d) pair production was assumed to be fixed (this is the parameter called parj (2) in PYTHIA, denoted as  $\lambda$  below). However, later experiments [7] have shown that this suppression decreases with increasing reaction energy. In Ref. [8], a reduction mechanism for the strange quark suppression has been introduced in the LUCIAE model. Using this mechanism, they were able to successfully describe the strangeness enhancement in pp, pA, and AA collisions at CERN Super Proton Synchrotron (SPS) energies [8, 9].

In order to study the strange particle production and strangeness enhancement in relativistic pp collisions, we have previously introduced a reduction mechanism for strange quark suppression in the PACIAE model [10, 11]. In this paper, we will use this reduction mechanism for strange quark suppression to investigate relativistic nucleus-nucleus collisions in the RHIC and Large Hadron Collider (LHC) energy regions.

This paper is organized as follows. In Section 2 we will give a brief review of the PACIAE model and the reduction mechanism for strange quark suppression. In Section 3 we will use the parton and hadron cascade model PACIAE to systematically analyze the strangeness production in Au+Au collisions at RHIC energies and Pb+Pb collisions at LHC energies. Section 4 gives a summary and conclusion.

Received 15 June 2013, Revised 27 August 2013

<sup>\*</sup> Supported by National Natural Science Foundation of China (11247021, 10975091), Excellent Youth Foundation of Hubei Scientific Committee (2006ABB036) and Key Laboratory Foundation of Quark and Lepton Physics (Hua-Zhong Normal University) (QLPL201101)  
1) E-mail: fengsq@ctgu.edu.cn

©2014 Chinese Physical Society and the Institute of High Energy Physics of the Chinese Academy of Sciences and the Institute of Modern Physics of the Chinese Academy of Sciences and IOP Publishing Ltd

## 2 The new modified PACIAE model

Based on PYTHIA [12], the parton and hadron cascade model PACIAE is a model not only for elementary collisions, but also for nucleus-nucleus collisions. The PACIAE model consists of four stages: parton initialization, parton evolution (rescattering), hadronization, and hadron evolution (rescattering), which are described below:

(1) Parton initialization: In the PACIAE model, a nucleus-nucleus collision is decomposed into nucleon-nucleon (NN) collisions based on the collision geometry. A NN collision is described by the PYTHIA model, where a hadron-hadron (h-h) collision is decomposed into the parton-parton collisions, with the string fragmentation (hadronization) process switched off. One then obtains a parton configuration composed of quarks, antiquarks, and gluons, besides a few hadronic remnants for a h-h collision after diquarks (anti-diquarks) have been split randomly into quarks (anti-quarks). This parton configuration is regarded as QGP formed in the initial state of h-h collisions.

(2) Parton evolution (rescattering): Rescattering among the QGP partons is then considered by the 2→2 LO-pQCD parton-parton cross sections [13]. The differential cross section of a subprocess  $ij \rightarrow kl$  is

$$\frac{d\sigma_{ij \rightarrow kl}}{d\hat{t}} = K \frac{\pi\alpha_s^2}{\hat{s}} \sum_{ij \rightarrow kl}, \quad (1)$$

where the factor  $K$  is introduced to compensate for higher order and non-perturbative corrections,  $\alpha_s=0.47$  stands for the effective strong coupling constant, and  $\hat{s}$ ,  $\hat{t}$  and  $\hat{u}$  refer to the Mandelstam variables. Taking the process  $q_1q_2 \rightarrow q_1q_2$  as an example, one has

$$\sum_{q_1q_2 \rightarrow q_1q_2} = \frac{4}{9} \frac{\hat{s}^2 + \hat{u}^2}{\hat{t}^2}. \quad (2)$$

This is regularized by introducing the parton color screen mass  $\mu=0.63$  GeV, giving

$$\sum_{q_1q_2 \rightarrow q_1q_2} = \frac{4}{9} \frac{\hat{s}^2 + \hat{u}^2}{(\hat{t} - \mu^2)^2}. \quad (3)$$

The total cross section of parton collision  $i+j$  is then

$$\sigma_{ij}(\hat{s}) = \sum_{k,l} \int_{-\hat{s}}^0 d\hat{t} \frac{d\sigma_{ij \rightarrow kl}}{d\hat{t}}. \quad (4)$$

The total and differential cross sections for the parton evolution (rescattering) can then be simulated by the Monte Carlo method until all parton-parton collisions are exhausted (partonic freeze-out). The results introduced below were calculated using these pQCD cross sections, except for those specially mentioned.

(3) Hadronization: The parton evolution stage is followed by hadronization at the moment of partonic freeze-out (no more parton collisions). In the hadronization stage, the partonic matter can be hadronized by the LUND string fragmentation model [12] or by the Monte Carlo coalescence model. The LUND string fragmentation model is adopted in this paper.

(4) Hadron evolution (rescattering): After hadronization, rescattering among the hadrons produced is modeled with the usual two-body collision model. The rescatterings among  $\pi$ , K, p, n,  $\rho(\omega)$ ,  $\Delta$ ,  $\Lambda$ ,  $\Sigma$ ,  $\Xi$ ,  $\Omega$ , J/ $\Psi$  and their antiparticles are considered for the moment. The isospin averaged parametrization formula [14, 15] is assumed for the cross section of h-h collisions. In addition, some constant total cross sections ( $\sigma_{\text{tot}}^{\text{NN}}=40$  mb,  $\sigma_{\text{tot}}^{\pi\text{N}}=25$  mb,  $\sigma_{\text{tot}}^{\text{KN}}=20$  mb and  $\sigma_{\text{tot}}^{\pi\pi}=10$  mb) and the ratio of inelastic to total cross section (0.85) are assumed and provided as another option.

In the LUND string fragmentation regime, the  $q\bar{q}$  pair with quark mass  $m$  and transverse momentum  $p_T$  may be created quantum mechanically at one point and then tunneled out to the classically allowed region. This tunneling probability is given by

$$\exp\left(-\frac{\pi m^2}{\kappa}\right) \exp\left(-\frac{\pi p_T^2}{\kappa}\right), \quad (5)$$

where the string tension is assumed to be a constant of  $\kappa \approx 1$  GeV/fm  $\approx 0.2$  GeV<sup>2</sup> [6, 12]. This probability implies a suppression of strange quark production  $u:d:s:c \approx 1:1:0.3:10^{-11}$ . The charm and heavier quarks are not expected to be produced in the soft string fragmentation process, provided no charm and heavier quarks appear in the string, but only in the hard process or as part of the initial- and final-state QCD radiations. Provided that the string tension is large, the higher  $p_T$  quark pair is expected to be created.

A mechanism for the increase in effective string tension and, hence, the reduction of strange quark suppression was introduced in Ref. [8]. In that paper, it was assumed that the effective string tension increases with the increase in number and the hardening of gluons in the string according to

$$\kappa^{\text{eff}} = \kappa_0(1-\xi)^{-\alpha}, \quad (6)$$

$$\xi = \frac{\ln\left(\frac{k_{T\text{max}}^2}{s_0}\right)}{\ln\left(\frac{s}{s_0}\right) + \sum_{j=2}^{n-1} \ln\left(\frac{k_{Tj}^2}{s_0}\right)}, \quad (7)$$

where  $\kappa_0$  is the string tension of the pure  $q\bar{q}$  string, which is assumed to be  $\sim 1$  GeV/fm. The gluons in the multi-gluon string are ordered from 2 to  $n-1$  because the two ends of the string are quark and antiquark.  $k_{Tj}$  is the transverse momentum of gluon  $j$  with  $k_{Tj}^2 \geq 0$  and  $k_{T\text{max}}$

is largest gluon transverse momentum in the string. The parameters  $\alpha=3.5$  GeV and  $\sqrt{s_0}=0.8$  GeV are determined by fitting h-h collision data. It should be mentioned that Eq. (8) represents the scale of the deviation of the multi-gluon string from the pure string.

In the PYTHIA model, there are four adjustable parameters:

parj (1) is the suppression of diquark-antidiquark pair production compared to quark-antiquark production;

parj (2) is the suppression of s quark pair production compared to u or d pair production;

parj (3) is the extra suppression of strange diquark production compared to the normal suppression of strange quarks; and,

parj (21) corresponds to the width  $\sigma$  in the Gaussian  $p_x$  and  $p_y$  transverse momentum distributions for primary hadrons.

The corresponding parameters can easily be found in the PACIAE model. They can be tuned to reduce the strange quark suppression and to change the width of its  $P_T$  distribution.

If  $\lambda$  denotes parj (2), then by Eq. (6) we can obtain

$$\lambda_2 = \lambda_1 \frac{\kappa_1^{\text{eff}}}{\kappa_2^{\text{eff}}}, \quad (8)$$

$$\sigma_2 = \sigma_1 \left( \frac{\kappa_2^{\text{eff}}}{\kappa_1^{\text{eff}}} \right)^{1/2}, \quad (9)$$

where the same subscript indicates the same string, and  $\kappa_1^{\text{eff}}$  ( $\kappa_2^{\text{eff}}$ ) is the effective string tension in Eq. (7). It is not hard to prove that Eq. (9) is also valid for parj (1) and parj (3).

The reduction mechanism for strange quark suppression has been included in the PACIAE model (setting parameter  $\text{kjp22}=1$ ). One can first tune the parameters parj (1), parj (2), and parj (3) (in this paper, we assume that parameter parj (21) is a constant) to fit the strangeness production data for a given nuclear collision system at a given energy. The resulting parj (1), parj (2), and parj (3) can be used to predict the strangeness production in the same reaction system at different energies, and even in different reaction systems.

### 3 Calculations and results

Default values for the model parameters in PACIAE were set according to experimental measurements and/or physics arguments [4]. However, for specific calculations a few sensitive parameters, such as  $K$ ,  $\beta$  and  $\Delta t$  in this paper, should be tuned to a datum of the global measurable, for instance, the charged multiplicity or the charged particle rapidity density at mid-rapidity. The fitted parameters can then be used to investigate the other physical observables.

In this paper, the parameter  $K$ , which was mentioned in Section 2, is introduced to account for higher order and non-perturbative corrections to the LO-pQCD parton-parton differential cross section; the parameter  $\beta$  is from the LUND string fragmentation function; and the parameter  $\Delta t$  is the smallest time interval of two distinguishably consecutive collisions in the parton initiation stage.

The parameters  $K$ ,  $\beta$  and  $\Delta t$  were first tuned to suitable values, making the charged multiplicity or the charged particle rapidity density at mid-rapidity of each centrality bin calculated by the PACIAE model fit to the global measurable. We then tuned the parameters parj (1), parj (2), parj (3) to a datum of the experiment results, such as the yields of strange particles. The fitted parameters were then used to investigate the other physical observables; for instance, the transverse momentum distribution in this paper.

We first globally tuned the parameters parj (1), parj (2), and parj (3) in PACIAE simulations to fit the strangeness production data from Au+Au collisions at  $\sqrt{s_{\text{NN}}}=200$  GeV. The yields of strange particles calculated by PACIAE compared to the STAR results are shown in Table 1. From Table 1, we can see that the data for strange particle yields from the STAR collaboration are reproduced well by PACIAE with the reduction mechanism for strange quark suppression.

The transverse momentum distributions ( $0 < p_T < 6$ ) of strange particles in the relativistic Au+Au collisions at  $\sqrt{s_{\text{NN}}}=200$  GeV are shown in Fig. 1, with the corresponding STAR data taken from Ref. [3]. Panels (a),

Table 1. Strange particle rapidity densities at midrapidity ( $|y| < 0.5$ ) in relativistic Au+Au collisions at  $\sqrt{s_{\text{NN}}}=200$  GeV. The STAR data are taken from Ref. [3].

centrality	$dN/dy$					
	$K_S^0$		$\Lambda$		$\bar{\Lambda}$	
	STAR	PACIAE	STAR	PACIAE	STAR	PACIAE
0-5%	43.5±2.4	43.66	14.8±1.5	16.04	11.7±0.9	12.01
10%-20%	27.8±1.4	27.57	9.16±0.89	9.84	7.27±0.55	7.30
20%-40%	16.5±0.83	16.18	5.70±0.55	5.74	4.53±0.34	4.21
40%-60%	7.26±0.49	6.91	2.38±0.23	2.32	1.82±0.14	1.83
60%-80%	2.14±0.19	2.09	0.71±0.07	0.68	0.55±0.04	0.54

(b), and (c) in Fig. 1 are for  $K_S^0$ ,  $\Lambda$ , and  $\bar{\Lambda}$  respectively. In order to present the results at different centralities in the same plot, we multiply the data at 0–5%, 10%–20%, 20%–40%, 40%–60% and 60%–80% by  $10^0$ ,  $10^2$ ,  $10^4$ ,  $10^6$  and  $10^8$ , respectively. These results indicate that the STAR data for strange particle transverse momentum spectra is well described by PACIAE.

Furthermore, looking at the data for charged particle rapidity density at mid-rapidity [16], we tuned the parameters of  $K$ ,  $\beta$  and  $\Delta t$  to fit the data at each centrality bin. We used PACIAE to study the results

of strange particle productions in Pb+Pb collisions at  $\sqrt{s_{NN}}=2.76$  TeV [2]. The transverse momentum distributions ( $0 < p_T < 6$  GeV/c) of the  $K_S^0$  and  $\Lambda$  particles at ALICE are shown in Fig. 2(a, b), respectively. In order to present the results at different centralities in the same plot, we multiply the data at 0–10%, 10%–20%, 20%–40%, 40%–60% and 60%–80% by  $4.0 \times 10^0$ ,  $2.0 \times 10^2$ ,  $1.5 \times 10^4$ ,  $10^6$  and  $10^8$ , respectively. From Fig. 2, we can see that the ALICE data for strange particle transverse momentum spectra can also be well described by PACIAE.

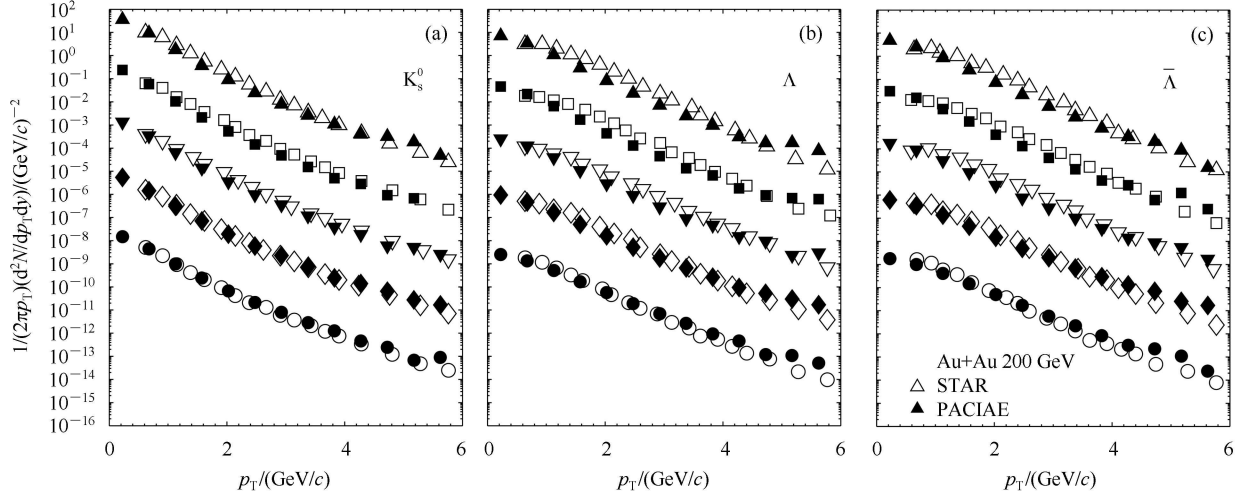


Fig. 1. The transverse momentum distributions of strange particles in relativistic Au+Au collisions at  $\sqrt{s_{NN}}=200$  GeV. Panels (a), (b), and (c) are for  $K_S^0$ ,  $\Lambda$ , and  $\bar{\Lambda}$ , respectively. The STAR data are taken from Ref. [3].

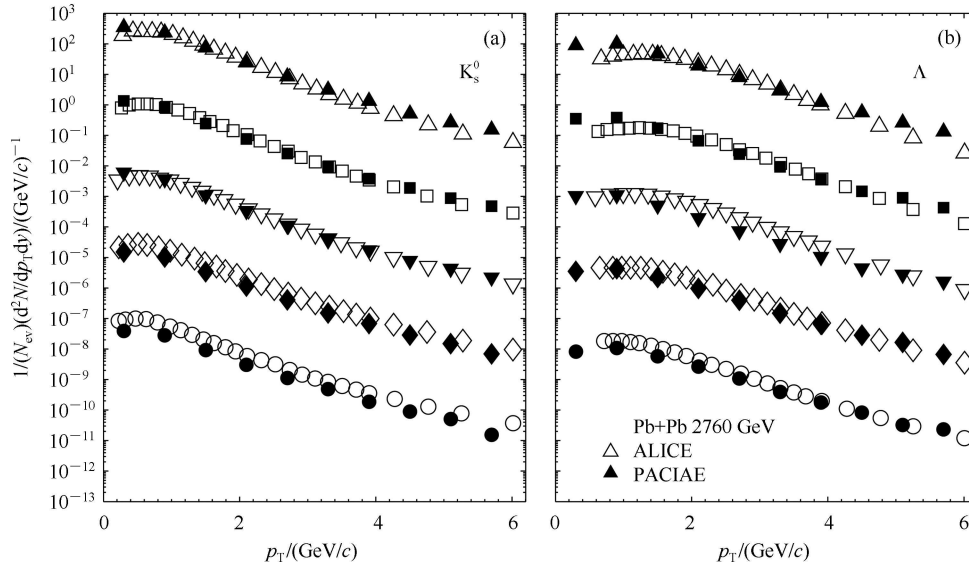


Fig. 2. The transverse momentum distributions of strange particles in relativistic Pb+Pb collisions at  $\sqrt{s_{NN}}=2.76$  TeV. Panels (a), and (b) are for  $K_S^0$ , and  $\Lambda$ , respectively. The ALICE data are from Ref. [2].

## 4 Conclusions

In summary, we have utilized the PACIAE model with the reduction mechanism for strange quark suppression to analyze strange particle production in relativistic Au+Au collisions at  $\sqrt{s_{NN}}=200$  GeV and Pb+Pb collisions at  $\sqrt{s_{NN}}=2.76$  TeV. The PACIAE results for the strange particle rapidity densities at midrapidity ( $|y| < 0.5$ ) and transverse momentum distributions ( $0 < p_T < 6$  GeV/c) are compared with STAR data and ALICE data, respectively. We find that, in general, the PACIAE model with the reduction mechanism for strange quark suppression describes the experimental data very well.

In Ref. [4, 10], we demonstrated that the effect of the reduction mechanism for strange quark suppression and the parton and hadron re-scatterings introduced in the

modified PACIAE model are reasonable for pp collisions at RHIC and LHC energy region. Here, it is found that the effect of the reduction mechanism of strange quark suppression and the parton and hadron re-scatterings are also reasonable for nuclear-nuclear collisions at RHIC and LHC energy regions.

In this paper, we used PACIAE to study only some of the strange particle productions, such as  $K_S^0$ ,  $\Lambda$ , and  $\bar{\Lambda}$ , because their yields are larger than other strange particles, such as  $\Xi^-$ ,  $\Omega^-$ , and their antiparticles. In order to further study the strangeness production mechanism, we also need to check the strangeness production mechanisms of  $\Xi^-$ ,  $\Omega^-$  and their antiparticles. We will do this further research in our next work.

*We thank Prof. Sa Ben-Hao for his valuable discussions and very helpful suggestions.*

## References

- 1 Rafelski J, Möller B. Phys. Rev. Lett., 1982, **48**: 1066
- 2 Chinellato D D. (ALICE collaboration). arXiv: 1211.7298
- 3 Agakishiev G (Dubna, JINR) et al. (STAR collaboration), Phys. Rev. Lett., 2012, **108**: 072301
- 4 SA Ben-Hao, ZHOU Dai-Mei, YAN Yu-Liang, LI Xiao-Mei, FENG Sheng-Qin, CAI Xu. Comput. Phys. Commun, 2012, **183**: 333-346
- 5 SA Ben-Hao, ZHOU Dai-Mei, DONG Bao-Guo, YAN Yu-Liang, MA Hai-Liang, LI Xiao-Mei. J. Phys. G: Nucl. Part. Phys., 2009, **36**: 025007; YAN Yu-Liang, ZHOU Dai-Mei, DONG Bao-Guo, LI Xiao-Mei, MA Hai-Liang, SA Ben-Hao. Phys.Rev. C, 2012, **81**: 044914; ZHOU Dai-Mei, YAN Yu-Liang, DONG Bao-Guo, LI Xiao-Mei, WANG Du-Juan, CAI Xu, SA Ben-Hao. Nucl.Phys. A, 2011, **860**: 68
- 6 Andersson B, Gustafson G, Ingelman G, Sjöstrand T. Phys. Rep., 1983, **97**: 31
- 7 Bocquet G et al. (UA1 collaboration). Phys. Lett. B, 1996, **366**: 447
- 8 TAI An, SA Ben-Hao. Phys. Lett. B, 1997, **409**: 393
- 9 TAI An, SA Ben-Hao. Phys. Rev. C, 1998, **57**: 261
- 10 LONG Hai-Yan, FENG Sheng-Qin, ZHOU Dai-Mei, YAN Yu-Liang, MA Hai-Liang, SA Ben-Hao. Phys. Rev. C, 2011, **84**: 034905
- 11 LONG Hai-Yan, FENG Sheng-Qin. Chin. Phys. C (HEP & NP), 2012, **36**: 616
- 12 Sjöstrand T, Mrenna S, Skands P. J. High Energy Phys., 2006, **05**: 026
- 13 Combridge B L, Kripfgang J, Ranft J. Phys. Lett. B, 1977, **70**: 234
- 14 Koch P, Müller B, Rafelski J. Phys. Rep, 1986, **142**: 167
- 15 Baldini A et al. Total Cross Sections for Reactions of High Energy Particles. Berlin: Springer-Verlag, 1988
- 16 Abelev Betty (LLNL, Livermore) et al. (ALICE collaboration). arXiv: 1303.0737